

# Supporting Information

## Cattle, Clean Water, and Climate Change: Policy Choices for the Brazilian Agricultural Frontier

**Andrew Reid Bell, Maria Carmen Lemos, and Donald Scavia**

**19 Pages**  
**12 Figures**  
**2 Tables**

# Appendix A

## Systems Dynamics Causal Model Description

The causal model that is the basis for the SDM implemented in this study begins with the variable ‘Land in use for Cattle’ (Figure S1). The rancher puts more land into use for cattle, making available more grass and raising a greater number of cattle. This brings in more revenue, and raises profits – profits that encourage the rancher to reinvest in the land and develop more pasture (a reinforcing loop). At the same time, changing the land use and raising cattle both incur costs, mediating the rancher’s profits (a balancing loop). Land use for cattle means that land is taken out of forest or riparian buffer. It also means more overland flow, as the pastures soils get compacted. These two factors lead to more sediment load and pollution in surface waters. In this model, there are two possible sanctions to minimize this pollution – fines for insufficient forest/buffer, and charges for cleaning polluted volumes of water (both balancing loops). Finally, climate variability affects how well grass is produced, and can augment the volume of overland flow, leading to increased pollution and sanctions. Less grass means that our rancher needs to pay more to supplement the cattle diet, and together with augmented pollution, these effects diminish profitability of the ranch.

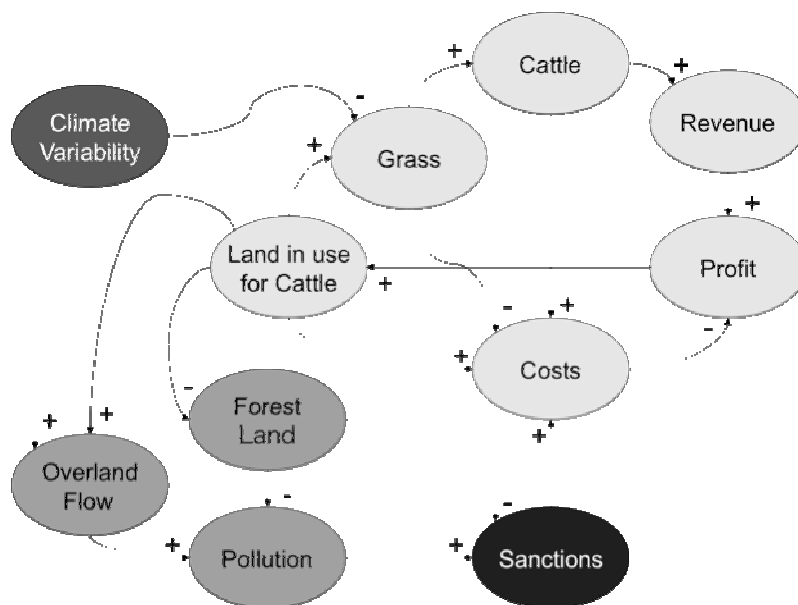
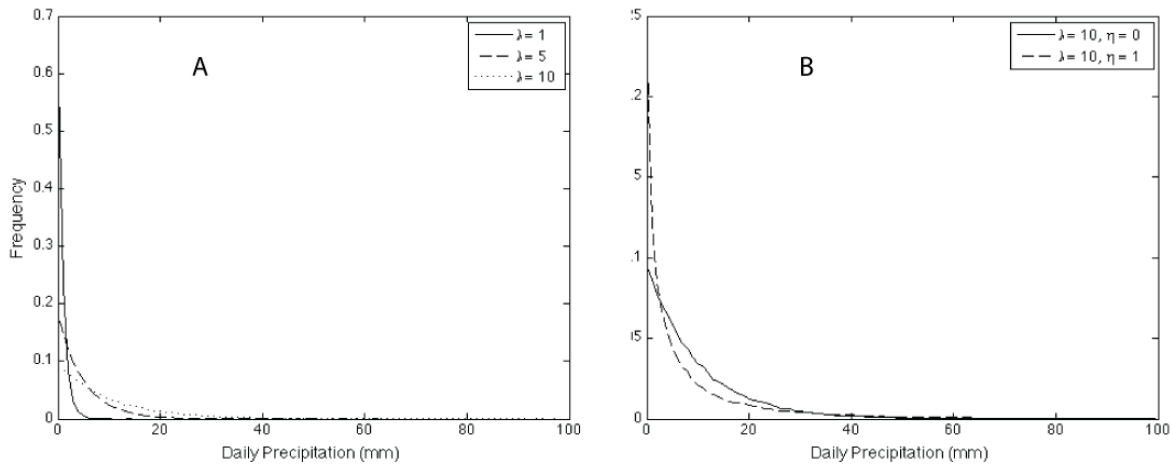


Figure S1 - Causal Model for Ranching/Water Pollution Coupled Natural-Human System

# Appendix B

## Distributions for Climate Model

Examples of the exponential distribution upon which the simple climate model is based are shown below in Figure S2A:



**Figure S2 – Examples of A) the basic exponential distribution and B) the exponential distribution modified by the parameter  $\eta$**

The parameter  $\eta$  modifies the exponential distribution by making extreme weather events more common without shifting the overall mean precipitation; that is, events in the long tail grow more frequent, as do the number of low- and zero-precipitation days (Figure 2B). Each of these curves was generated by plotting the histogram in bins of size 1 from 0 to 100, of 100000 draws from the following function:

$$\text{exprnd}(\text{lambda} * (1 - \eta) + \text{exprnd}(\eta * \text{lambda}))$$

for the values of  $\lambda$  and  $\eta$  indicated in the figure legends.

Monthly values of  $\lambda$  used in the modeling experiments, as well as the monthly values for potential evapotranspiration in forest and pasture, are given in Table S1.

**Table 1 - Monthly  $\lambda$  Values for Exponential Distribution**

| <b>Month</b> | <b><math>\lambda</math></b> | <b>Forest Potential ET</b> | <b>Pasture Potential ET</b> |
|--------------|-----------------------------|----------------------------|-----------------------------|
| January      | 10                          | 3.8                        | 3.6                         |
| February     | 6                           | 4                          | 3.6                         |
| March        | 5                           | 4.1                        | 3.5                         |
| April        | 4                           | 4.1                        | 3.4                         |
| May          | 2                           | 4                          | 3.2                         |
| June         | 1                           | 3.9                        | 3                           |
| July         | 1                           | 3.8                        | 2.9                         |
| August       | 2                           | 3.8                        | 2.7                         |
| September    | 6                           | 3.9                        | 2.5                         |
| October      | 8                           | 4.1                        | 2.6                         |
| November     | 9                           | 4.1                        | 3.2                         |
| December     | 10                          | 3.9                        | 3.4                         |

# Appendix C

## Systems Dynamics Model Parameters for Reference Mode

Where available and appropriate, literature values informed the parameter choices used in this model, with deviations from literature values noted below.

**Table S2: Model Parameters**

| Name            | Parameter Description                | Value        | Literature Values/Justifications                             |
|-----------------|--------------------------------------|--------------|--|
| $W_{calf}$      | Calf Weight                          | 50 kg        | Based on an adult weight of about 410kg [1]                  |
| $W_{2\ year}$   | Two-year Weight                      | 200 kg       |  |
| $W_{3\ year}$   | Three-year Weight                    | 400 kg       |  |
| $p$             | Price, Beef                          | \$3/kg       | \$R90/@ (15kg) [2]   |
| $C_{r,p}$       | Pasture Restoration Cost per hectare | \$300        | \$116-234/ha in 1991 [3]<br>\$260/ha in 1994 [1]             |
| $C_{r,f}$       | Forest Restoration Cost per hectare  | \$1,000      | \$2000/ha in São Paulo State [4]<br>\$800/ha in Amazonia [5] |
| $C_{c,f}$       | Forest Clearing Cost per hectare     | \$50         | Assumed  |
| $C_{nutrients}$ | Cost per kg Nutrient Supplement      | \$0.08       | Based on assumed grain prices of \$2-3/bushel                |
| $U_{daily,kg}$  | Nutritional Needs, Cattle            | 7 kg/100kg/d | 20-25kg/animal/d [6]   |
| $a_{change}$    | Maximum Land Use Change Rate         | 10 ha/y      | Assumed  |
| $A_{0,Buffer}$  | Nominal Width for minimal erosion    | 30-60 m      | Required width for rivers < 10m across [7]                   |

|                  |                                   |                |  |
|------------------|-----------------------------------|----------------|--|
| $Soil$           | Soil Water                        | 40 cm/m        | Assumed. Reasonable values estimated from SIGTERON Soil Profile database [8]   |
| $Capacity$       | Capacity                          |                |  |
| $SD$             | Soil Depth                        | 0.5-2m         |  |
| $R/L$            | Slope Grade                       | 5%             |  |
| $K_{Infilt,f}$   | Soil Infiltration Rate, Forest    | 1500 mm/h      | 1533 mm/h [9]  |
| $K_{Infilt,p}$   | Soil Infiltration Rate, Pasture   | 120 mm/h       | 122 mm/h [9]   |
| $K_{sat,f}$      | Saturation velocity, Forest       | 200 mm/h       | 206 mm/h [9]   |
| $K_{sat,p}$      | Saturation velocity, Pasture      | 20 mm/h        | 26 mm/h [9]  |
| $l$              | Mean Rain Event Length            | 1 h            | An operational variable to generate realistic hourly rainfall intensities from modeled daily rainfall distributions. Estimated from precipitation data for Ji-Paraná [10]          |
| $e_{0,p}$        | Nominal Erosion, Pasture          | 5 t/ha/y       | Based on erosion rates of 30 t/ha/y [11] up to 200 t/ha/y [12] for fields with exposed soils in São Paulo State, and erosion rates as low as 2 t/ha/y for maintained pastures [11] |
| $e_{0,dp}$       | Nominal Erosion, Degraded Pasture | 30 t/ha/y      |  |
| $k_{grass, max}$ | Intrinsic Grass Growth Rate       | 370 kg DM/ha/d | Chosen to give a capacity of about 1.5-2.0 head/hectare. Average stocking rates for Amazonia range from 0.5-1 [1, 3] head/hectare up to 6 head/hectare [13]                        |
| $G_0$            | Nominal Grazing Rate              | 60 kg/ha/d     |  |
| $S_{grass}$      | Pasture Grass Capacity            | 4000 kg/ha     |  |
| $n_0$            | Nominal Pasture Lifetime          | 10 years       | 5-10 years [1]   |
| $A_{plot}$       | Plot Size                         | 200 ha         | Assumed  |
| $w$              | Plot Width                        | 500 m          | Assumed  |
| $dt$             | Decision Interval                 | 1 y            | Assumed  |
| $r$              | Discount Rate                     | 10%            | Assumed  |

# Appendix D

## Full Systems Dynamics Model Results

### Typical Runs – BWC and LUF

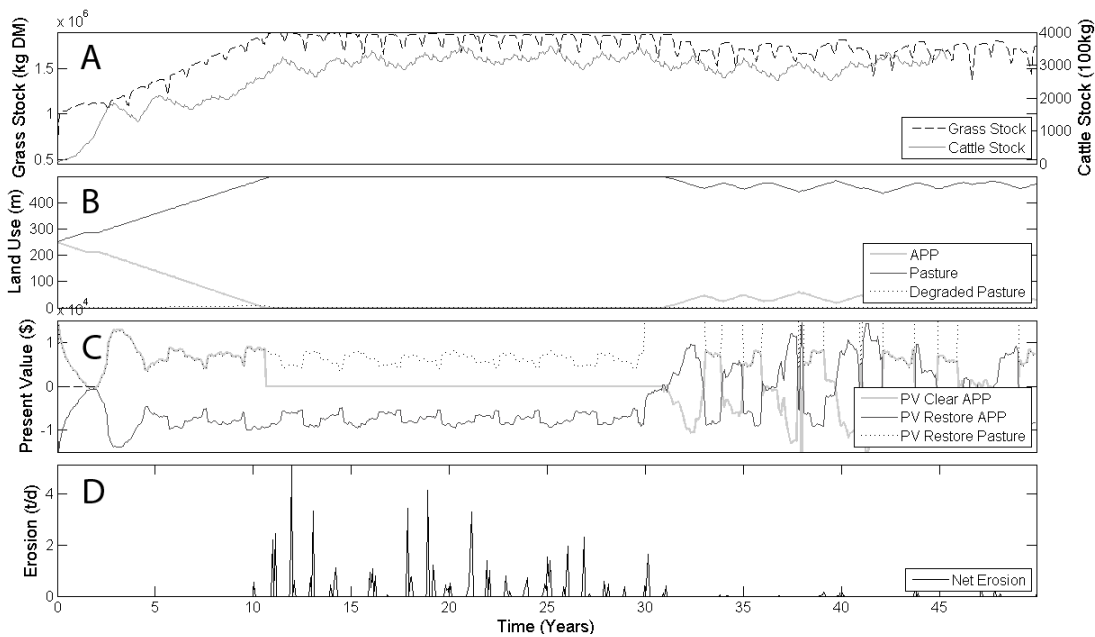


**Figure S3 - Typical Run for BWC with  $L_R = 0.0001 \text{ t/m}^3$  and  $S_{BW} = \$0.12/\text{m}^3$**

In each simulation, the model is run for a startup period of 20 years, during which time the ranching operation grows to a pseudo-steady state, and an additional 10 years at this pseudo-steady state. At 30 years, the fine is imposed, and the simulation continued for a further 20 years. All average results reported in this study are from the final 10 years of the simulation, where the rancher has had opportunity to respond to the imposed sanction.

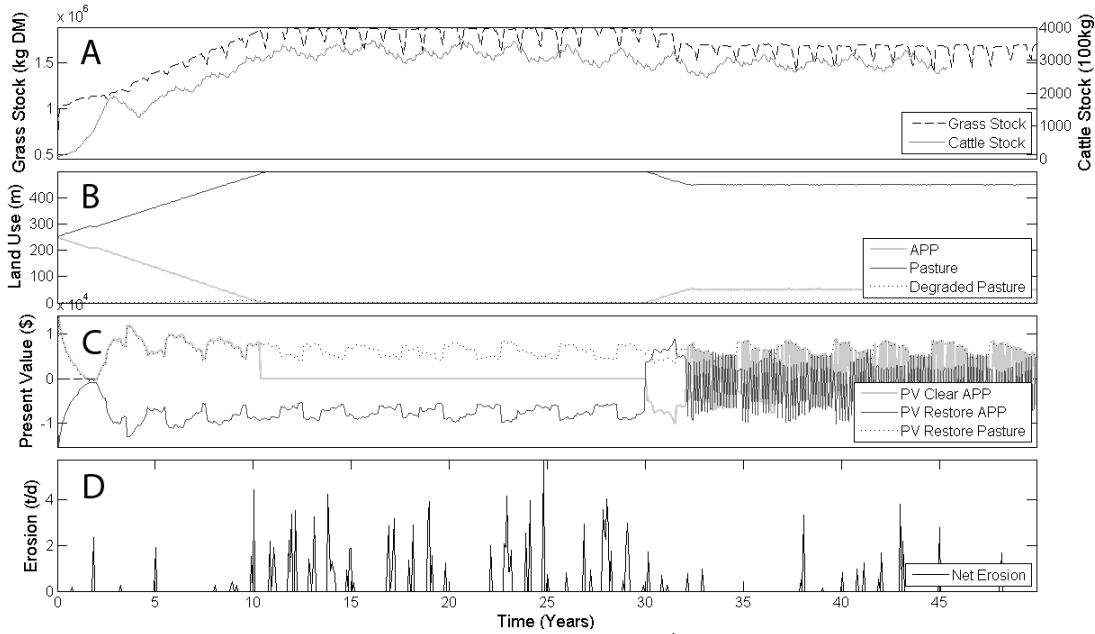


**Figure S4 - Typical Run for LUF with  $W_R = 50\text{m}$  and  $S_{LU} = \$3000/\text{ha}$**

During the startup period, the present value for pasture is consistently positive (Figure S3B and Figure S4B) and that for forest is negative, leading it to be completely converted to pasture by around year 10 (Figure S3C and Figure S4C). Without any forest, significant erosion occurs (Figure S3D and Figure S4D) – this can be thought of as the expected steady state result without any sanction in place. With the fine in place at year 30, the value of forest buffer land shifts, inducing the rancher to maintain more forest, and in turn reducing erosion (Figure S3D and Figure S4D). The high variability observed in the LUF run for the value of forest land, as compared with the BWC run, is due to the dramatic shift in the marginal value of forest as the width of the buffer hovers around  $W_R$ . The modeled land values, taken as the PV calculations in Figure S3C and Figure S4C, are consistent with measured land values for the basin. Sills and Caviglia-Harris found land values per hectare across the basin to vary from \$150 to \$10,000 per hectare [14].

### Approach 1 – Bulk Water Charges (BWC)

Increases to both unit sanctions for bulk water ( $S_{BW}$ ) and the sanction threshold ( $L_R$ ) cause smooth declines in profitability, although while  $S_{BW}$  is low this does not immediately shift practices and lead to reduced erosion rates (Figure S5A, Figure S5B). Above about  $S_{BW} = \$0.04/\text{m}^3$  in the simulation, the rancher begins to respond and both increases in unit sanction levels as well as decreases in sanction thresholds lead to smoothly decreases in net erosion (Figure S5B). These smooth shifts are the clear result of a rise in the average buffer width over the course of the simulation (Figure S5C) and significant pasture restoration such that levels of degraded pasture remain low across all cases (Figure S5D).



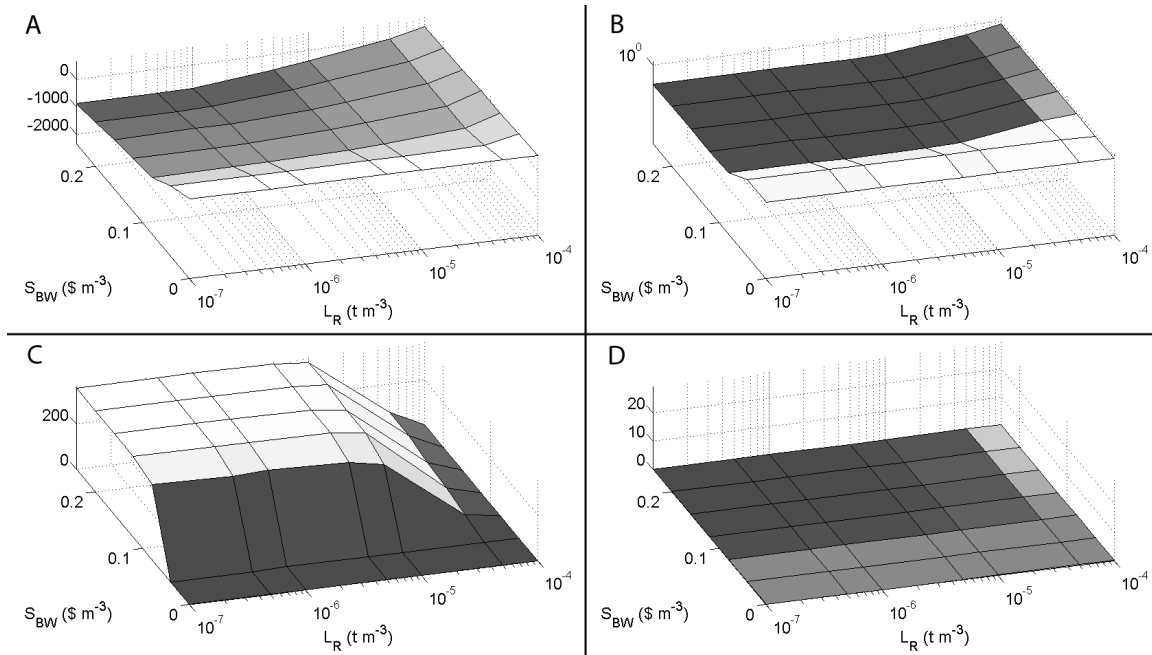


**Figure S5 – Response surfaces for BWC across sanction threshold  $L_R$  and unit sanction  $S_{BW}$ . A) Profit (\$/ha/y) B) Erosion (t/ha/y) C) Buffer Width (m) D) Degraded Pasture (m). Each point on the surface represents the mean profit per hectare over the final 10 years of the simulation, averaged across 100 Monte Carlo runs.**

## Approach 2 – Land Use Fines (LUF)

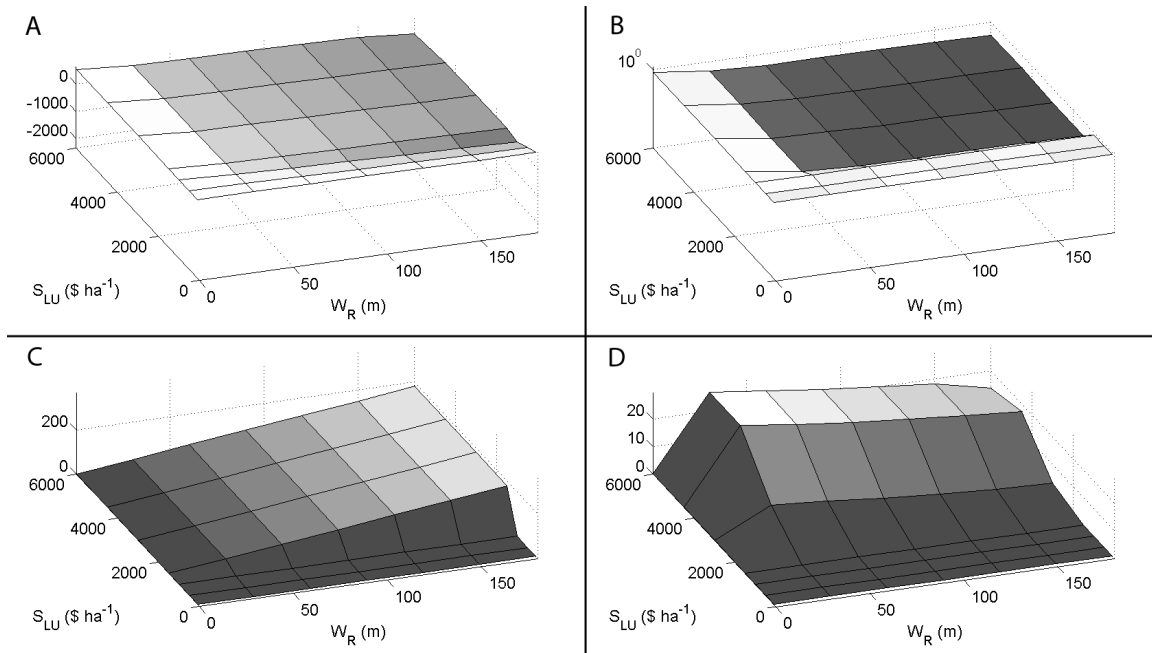


**Figure S6 - Response surfaces for LUF across sanction threshold  $L_R$  and unit sanction  $S_{BW}$ . A) Profit (\$/ha/y) B) Erosion (t/ha/y) C) Buffer Width (m) D) Degraded Pasture (m). Each point on the surface represents the mean profit per hectare over the final 10 years of the simulation, averaged across 100 Monte Carlo runs.**

As in the case for bulk water charges, low sanction ( $S_{LU}$ ) levels do not initially cause a change in behavior, and erosion levels do not shift (Figure S6B). However, above about  $S_{LU} = \$1000/\text{ha}$ , an abrupt ‘tipping point’ effect occurs as the rancher rapidly shifts his behavior to meet the target buffer width ( $W_R$ ) (Figure S6C). Further increases to  $S_{LU}$  above this value do not lead to further changes in the buffer width as the target  $W_R$  is already met; this target value appears to be achieved at the same value of  $S_{LU}$  across the set of simulations. Increases to  $W_R$  appear to lead to smooth decreases in net erosion in all cases where  $S_{LU}$  is above the ‘tipping point.’

### Contrasting BWC and LUF

A first key difference in the LUF case from the BWC approach is that increases in both  $W_R$  and  $S_{LU}$  from zero initially lead to significant rises in the amount of degraded pasture on the property (Figure S6D). Degraded pasture width peaks at about 25m (or about 5% of the property), and then declines with further increases in  $W_R$  as the total amount of pasture that can degrade declines. Since the LUF does not specifically reward reduction in pollution, only the maintenance of required buffer widths, the value of restoring pasture relative to its value in the BWC case is lower, and it accumulates. This occurrence is not unrealistic; Fearnside summarized estimates of pasture degradation in Amazonia ranging from 17% to 54% of total pasture area as recently as 1986 [15], and more recently estimated an equilibrium point for Amazonia of about 10% of pasture land in degradation [16].

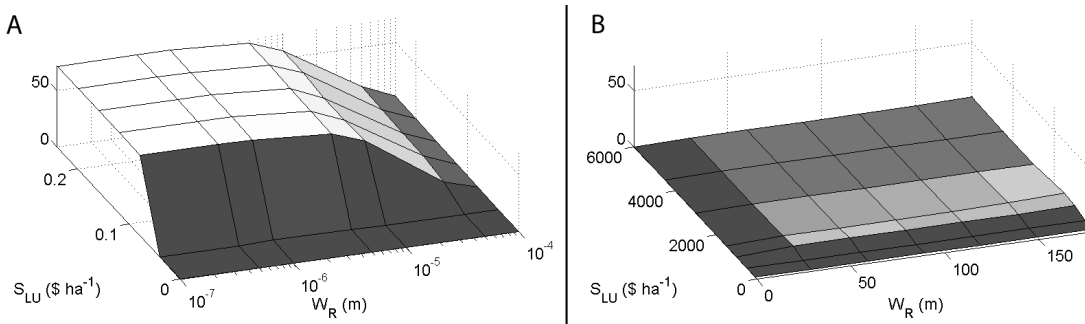


**Figure S7 - Standard Deviation in Buffer Width Over Time (m) for A) BWC and B) LUF across sanction threshold  $L_R$  and unit sanction  $S_{BW}$ . Each point on the surface represents the standard deviation in buffer width over the final 10 years of the simulation, averaged across 100 Monte Carlo runs.**

An important dynamic difference between the BWC and LUF scenarios in this simulation is the way in which buffers are maintained over time. In the LUF scenario, the required buffer width  $W_R$  is achieved quickly after the policy is implemented (Figure S4) and remains stable for the remainder of the simulation, such that the standard deviation of the buffer width across time late in the simulation is very low (Figure S7B). In contrast, the buffer widths in the BWC simulation are much more dynamically variable, leading to higher standard deviations over the final 10 years of the simulation (Figure S7A). Since climate and the rate of generation of overland flow, as well as the effectiveness of buffers in trapping eroded sediment are variable and not perfectly known to the rancher, a consistent and stable ‘optimal’ buffer width does not emerge within the simulation. The rancher ends up maintaining land more dynamically, planting wider buffers to reduce pollution charges and removing them as the opportunity cost for raising cattle rises.

Comparisons between these approaches is hampered by the fact that the policy dimensions are different in each case, and by the difficulty in viewing how these different outcomes – principally profitability and net erosion – co-vary within and across scenarios. To make comparison easier, we adopt the ‘sanction response curve’ as a means of representing components of the response surfaces shown above. Sanction response curves are explained in full in Appendix D.

### Sanction Response Curve – BWC

Looking along the curve of decreasing  $L_R$  at  $S_{BW} = \$0.24/\text{m}^3$ , a profile of the sanction response form in Figure S12 (Appendix D) is clear (Figure S8A). Since the constant high fine per unit of contaminated water along the entire curve creates some incentive to change behavior even at higher erosion thresholds, we do not observe a flat ‘Weak’ region. A smooth drop occurs in the ‘Effective’ region, bottoming out in the ‘Burden’ region.

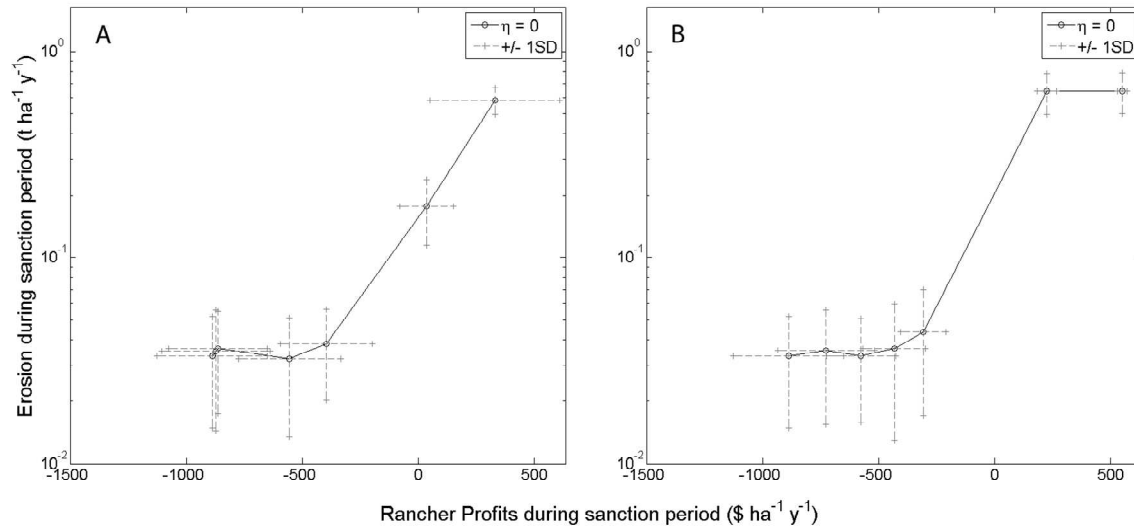


**Figure S8 - Sanction Response Curve across A) Constant Unit Sanction of  $S_{BW} = \$0.24/\text{m}^3$  and B) Constant Sanction Threshold of  $L_R = 10^{-6} \text{ t/m}^3$  for BWC. Grey dashed lines indicate the range of values observed in the Monte Carlo analysis; solid black circles indicate mean values across Monte Carlo runs.**

The ranges observed in both profitability and erosion in the Monte Carlo analysis (grey dashed lines in both Figure S8 and S9) reflect the significant environmental differences between runs in the Monte Carlo analysis and give confidence that we are evaluating these policy approaches over a truly rugged landscape – where high overland flow is coupled with ineffective riparian buffers in some instances, or where deep soil and thick riparian buffers keep erosion low in others. Even with these ranges, there is a clear statistical difference between the endpoints of the curves in Figures S8 and S9 for both erosion and profit outcomes, demonstrating the existence of distinct ‘Weak’ and ‘Burden’ regions, and implicitly, the ‘Effective’ regions that are the transitions between them.

The curve of increasing  $S_{BW}$  at a constant low threshold of  $L_R = 10^{-6} \text{ t/m}^3$  is more similar to that observed in Figure S12 (Figure S8B). A clear flat ‘Weak’ region is present, showing that at low

unit sanction levels, there is not a strong enough signal to influence behavior – that is, when the unit fine is low, the rancher prefers to pay the sanction rather than changing his practice.

### Sanction Response Curve – LUF

The LUF curves are distinctly different from those for BWC. First looking along the curve of increasing  $W_R$  at  $S_{LU} = \$9000/\text{ha}$ , like in the BWC constant  $S_{BW}$  case, erosion levels begin to drop immediately as  $W_R$  increases since with high  $S_{LU}$  there is a clear signal for the rancher to follow (i.e., it is always worthwhile for the rancher to try to change his practice) (Figure S9A).

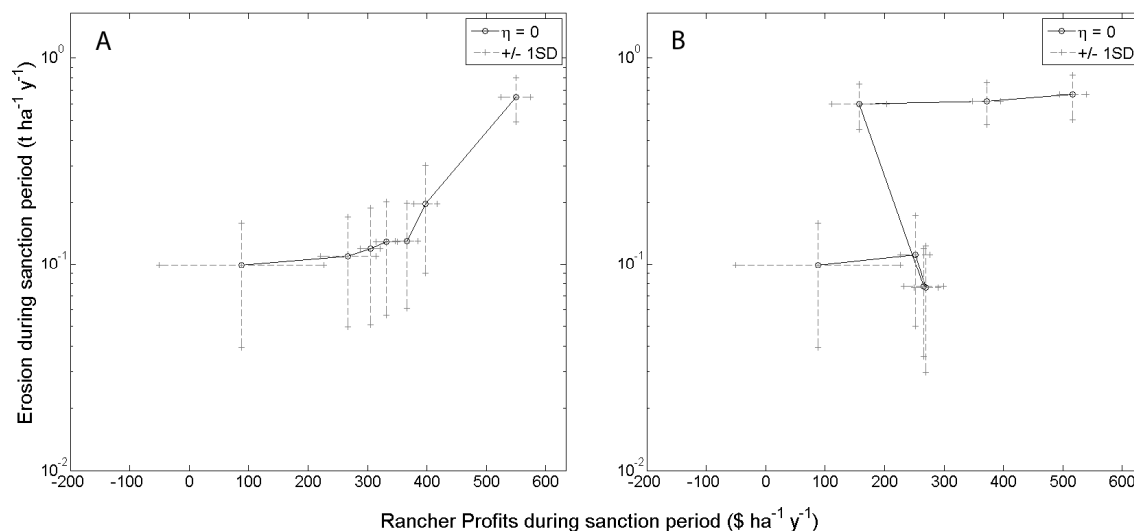


**Figure S9 - Sanction Response Curve across A) Constant Unit Sanction of  $S_{LU} = \$9000/\text{ha}$  and B) Constant Target Buffer Width of  $W_R = 180\text{m}$  for LUF. Grey dashed lines indicate the range of values observed in the Monte Carlo analysis; solid black circles indicate mean values**

The curve for constant  $W_R = 180\text{m}$  at increasing  $S_{LU}$  is distinct from the previous curves in that it shows the clearest ‘tipping point’ behavior of the group. A smooth decline in profitability without a change in erosion levels is then followed by a rapid drop in erosion and bump in profitability as  $S_{LU}$  crosses the threshold that moves the rancher from complete noncompliance to near complete compliance (Figure S9B). In other words, the high target buffer width is onerous enough that it takes a fairly significant sanction to encourage the rancher to adhere to it. Once he does, he experiences a bump in profitability as the drop in sanctioning outweighs the lost revenue. Several of the subsequent increases in  $S_{LU}$  bring about neither changes in profitability nor erosion, since the rancher is in complete compliance with regulations and does not change their behavior further. Beyond this point however, in the ‘Burden’ region, both profitability and environmental performance decline. This is a result of the higher rate at which the rancher acts to comply with the regulations when the sanction is particularly onerous. Since in the model the rancher does not sell cattle until they are 3 years of age, the turnover of land into buffer or degraded pasture crowds cattle into a smaller pasture area. A high enough cattle density causes the grass supply to be critically drained, and the production of cattle crashes. This model does not treat the re-establishment of ranching operations following a crash, so that profitability drops, and large tracts of degraded pasture are left, resulting in poorer environmental outcomes. This

particular outcome may not have a clear analog in reality – ranchers are likely to sell cattle early or otherwise adjust their behavior more radically to avoid crashing their pastures – and may simply be an artifact occurring at the limit of the model’s useful range. However, that it does occur does draw attention to the interaction between policy and dynamic systems – the severity of a sanction and the timescale over which it is implemented need to respect the capacity of sanctionees to adapt and react.

### **Contrasting BWC and LUF**

Comparing the absolute performance of the BWC and LUF along the sanction response curve, it is easily seen that BWC achieves better reduction of erosion, but at a much higher cost to the rancher (compare Figure S8 with Figure S9). Variability in climate and the relationships between soil, overland flow, and buffer effectiveness make it much more difficult for the rancher to minimize erosion than it is to comply with a simple land use regulation. By specifically targeting erosion outcomes, the BWC achieves better erosion reduction; however, by targeting an imperfect proxy for low erosion outcomes, a standardized buffer width, the LUF achieves a more modest reduction in erosion but preserves the livelihood of the rancher.

### **BWC and LUF as adaptations to Climate Change**

As climate grows more variable, ranchers are less able to judge how well grass will grow and thus how much cattle their land will support. Further, peak profits for ranchers are lower with higher climate variability, as the costs for nutrient supplements and other inputs during dry periods rise. When erosion is considered as well, the effects are more pronounced – greater overland flow brought about by severe storms [17] and by increased conversion to agricultural use [18] leads to greater erosion into surface waters and greater effects on downstream aquatic and human systems.

In the following sections, we investigate how the performances of BWC and LUF shift under changes in the climate, as measured through the social dimension of profitability and the environmental dimension of net sediment loading. Each of the curves in Figure 3 in the main article shows the policy response curves under 6 scenarios for climate – high ( $\eta = 1$ ) and low ( $\eta = 0$ ) variability cases for each of runs with lower ( $v = -10\%$ ), normal ( $v = 0$ ), and higher ( $v = +10\%$ ) precipitation. Scenarios corresponding to low and high variability are marked with circles and triangles, respectively, and scenarios corresponding to lower, normal, and higher precipitation are marked with dashed, solid, and dotted lines, respectively. Each curve within a figure is generated using the same policy parameters.

While the choice of  $v = \pm 10\%$  is based on the IPCC findings summarized in [19], the choice of  $\eta = (0, 1)$  is more arbitrary, since the expected change in the frequency of extreme weather events is less well known or reported, and is made for reasons of clarity and simplicity. Thus, it is important to emphasize that the two effects ( $\eta$  and  $v$ ) are not necessarily expected to scale against each other as they do in these simulations, and that these results should not imply that the change in variability will have a more or less severe impact on ranching than the change in precipitation.

### **Response to Climate Change – BWC**

The striking result from the curves in Figure 3 (in main article), across constant  $S_{BW}$  and  $L_R$ , is that as both overall precipitation and variability increase, the performance of the BWC degrades. Specifically, for a given set of policy parameters net erosion rises, and profitability for the rancher falls. Moving along the sanction response curves from the ‘Weak’ region to the ‘Burden’ region, the spread between any two given curves in the figure increases, indicating that the policy is more effective in one scenario than in the other. Further, this shows that the impacts of changes in precipitation and climate variability manifest themselves more under strong sanctions than under weak sanctions.

It is important to note at this point that the only growth impact of climate change incorporated into this simple model is a linear effect of precipitation on grass productivity [20], so that the shifts in profitability here are dominated by the imposed sanctions. To the extent that the growth rate of pasture grass is affected in more complicated ways by changes in climate, these profiles would be different.

### **Response to Climate Change – LUF**

Where the effect of climate on BWC was to elongate the sanction response curve along the profitability axis, the effect on LUF appears, if anything, to be to compress the curve. Across both constant  $S_{LU}$  and  $W_R$ , increases in variability and in precipitation appear to shift the sanction response curves directly up along the erosion dimension with little movement along the profitability dimension (Figure 3 in main article). This is not entirely surprising, since the sanction requirements for the rancher (to maintain a buffer width of  $W_R$ ) are invariant across changes in climate, and any shifts in profitability in the model would be expected to arise from the changing capacity of the pasture grass to support cattle. What is worth noting is that the magnitude of the upward shift due to increasing variability and precipitation appears similar to the magnitude of the upward shifts seen for BWC. That is, while the LUF demonstrates overall lower performance in reducing erosion in this model, it demonstrates an equivalent robustness against climate change, as compared to the BWC.

# Appendix E

## Sanction Response Curves

To make comparisons across the different policy approaches and climate scenarios in this study, we propose the following set of curves as archetypal economic and environmental responses to sanctioning. This archetype assumes that enforcement of the sanction is uniform across different sanctioning strengths, and that the sanctionnee is behaving optimally – that is, acting to maximize profitability – before sanctions are levied.

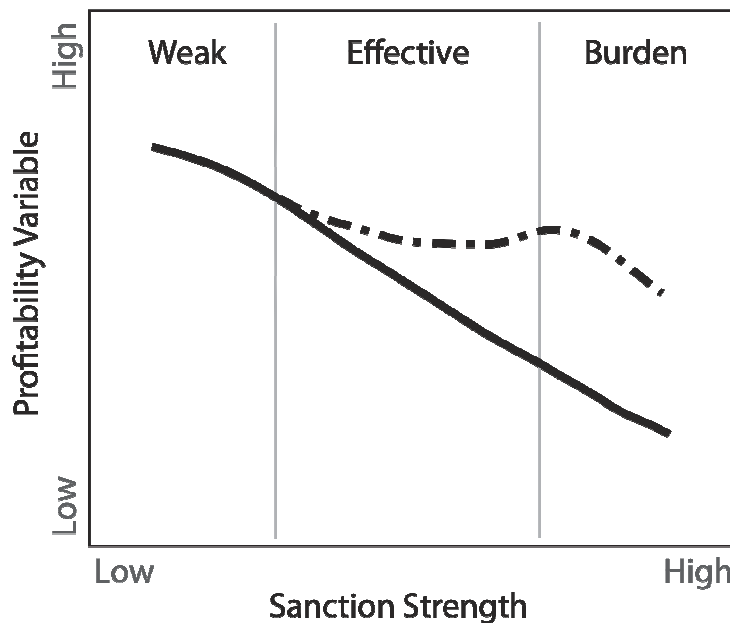


**Figure S10 - Profitability as a function of Sanction Strength**

In the most basic case, as sanctions are levied and become more severe, profitability will decline (Figure S10, solid line). At low strengths, sanctions may not be effective at shifting behavior and simply increase costs for the sanctionnee (Figure S10, solid line, 'Weak' region); at higher strengths, they may force the sanctionnee to change practices and the pollutant variable of interest may begin to decline (Figure S11, solid line, 'Effective' region). As sanctions become even stronger, the sanctionnee may reach the limit of changes that can be made, and further increases in

sanction strength simply increase the cost burden without further environmental improvement (Figures S10 and S11, solid line, ‘Burden’ region).

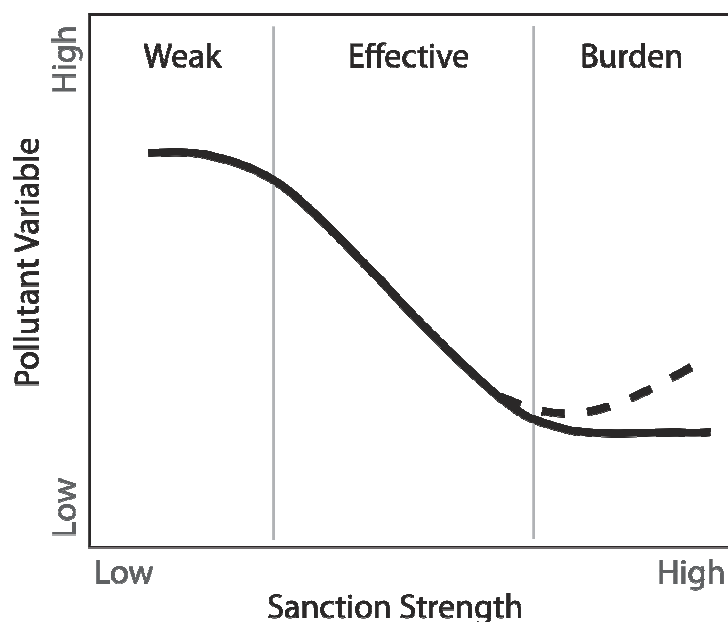


**Figure S11 - Pollution as a function of Sanction Strength**

However, there are important ways in which a sanction response may differ from this most basic case. In the first, an incremental increase in sanction strength may lead to a relative increase in profitability, if it causes the sanctionee to make some discrete change in practice that reduces pollution in such a way that the total sanctions levied are now lower than before (e.g., an addition to a chemical process that reduces generation of a harmful toxic byproduct to very low levels, but which is fairly expensive to install) – a threshold effect (Figure S10, dash-dotted line). In the second, sanctions that become too onerous may affect the ability of the sanctionee to maintain practices, leading to environmental degradation and a net increase in the pollutant variable with incremental increases to sanction strength e.g., the maintenance of wide riparian buffer zones such that the remaining pasture land can not support enough cattle to cover costs) (Figure S11, dashed line).

In our analysis, we are not focused on what pollution and profit outcomes are at particular sanction strengths. Across different policy approaches, sanction strengths cannot really be compared meaningfully, and the low-fidelity modeling approach of this paper means that calibration of sanction strengths should not be a goal. Instead, we are more interested in how the ranges of pollution and profit outcomes vary with each other and across scenarios. Thus, we propose in this paper to combine the information in Figure S10 and Figure S11 into a single ‘sanction response curve’ that plots pollution outcomes on the vertical axis against profitability outcomes on the horizontal axis (Figure S12).

In this distinctively sigmoidal or ‘S’-shaped curve, sanction strengths increase from right to left in the figure, corresponding to the same ‘Weak’, ‘Effective’, and ‘Burden’ regions as in Figure S10 and Figure S11. Rises in profitability due to threshold shifts in behavior brought about by



increased sanction strength manifest as inflection points on the horizontal axis (Figure S12, dash-dotted line); rises in pollution brought about by overly onerous sanctions and reduced capacity to manage pollution manifest as inflection points in the vertical axis (Figure S12, dashed line).

We propose this sanction response curve as a means of clearly representing the following properties of a sanction response on a single curve: 1) threshold behavior changes (such as discrete jumps in compliance or changes in technology that lead to improved profitability) as inflections in profitability variables, 2) overly onerous sanctions (such as a sanction that leaves ranchland unprofitable and in degradation) as inflections in pollution variables, as well as 3) the change in profitability over the effective behavior-changing range of the sanction ('Effective' region in Figures S10-S12). We apply it in this study to compare responses across approaches and climate scenarios.

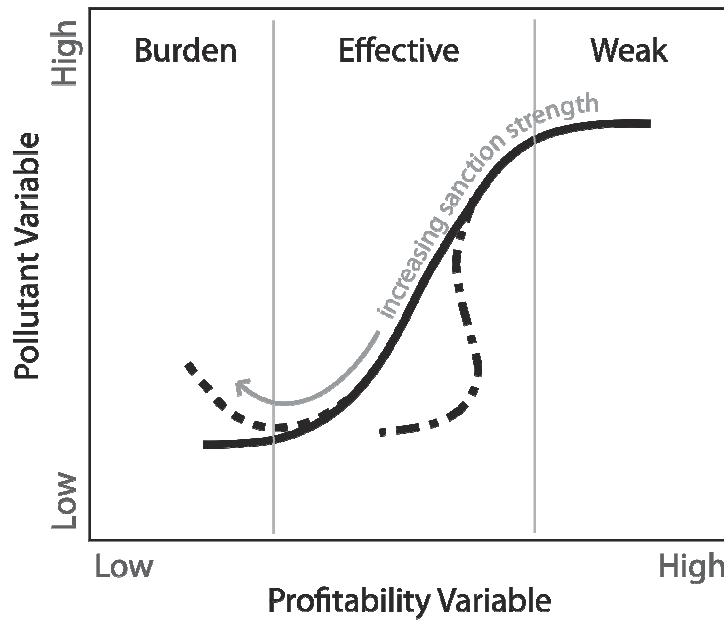


**Figure S12 - Sanction response curve across pollutant and profitability variables**

To reduce the data and make it more tractable in the main article, we selected slices of the previously shown response surfaces to generate the sanction response curves. We selected the most stringent slices along each dimension, holding the other dimension constant ( $S_{LU} = \$9000/\text{ha}$  and  $W_R = 180\text{m}$  for the LUF case,  $L_R = 1\text{e-}6 \text{ t/m}^3$  and  $S_{BW} = \$0.24/\text{m}^3$  for the BWC case). In other words, these slices are the model results along the back edges of the response surfaces in Figure S5 and Figure S6 (Appendix D). They represent extreme values for the policy dimensions where the burden of the sanction is particularly onerous and responses can be expected to be strong; finding results in the 'Burden' region shown in Figure S12 along both of these slices, where no further improvements to environmental outcomes is occurring, gives some confidence that the simulations have covered the regions in the possibility space defined by the two dimensions of the policy approach with the best erosion outcomes.

## LITERATURE CITED

1. Mattos, M.; Uhl, C., Economic and Ecological Perspectives on Ranching in the Eastern Amazon. *World Development* **1994**, 22, (2), 145-158.
2. Pecuária.com.br Pecuária.com.br. <http://www.pecuaria.com.br/> (January 15),
3. Smith, N. J. H.; Serrão, E. A. S.; Alvim, P. T.; Falesi, I. C., *Amazonia - Resiliency and Dynamism of the Land and its People*. United Nations University Press: Tokyo, Japan, 1995; p 268.
4. GEF *GEF Project Document on a Proposed Grant fro the Global Environment Facility Trust Fund in the amount of USD 7.75 Million to the State of São Paulo for a Ecosystem Restoration of Riparian Forests in São Paulo Project*; Global Environment Facility: April 15, 2005; p 132.
5. Fearnside, P. M., Land-tenure issues as factors in environmental destruction in Brazilian Amazonia: The case of Southern Para. *World Dev.* **2001**, 29, (8), 1361-1372.
6. NRC, Dry Matter Intake. In *Nutrient Requirements of Dairy Cattle*, 7 ed.; National Academy Press: Washington, D.C., USA., 2001; p 408.
7. Brasil, F. R. o., Código Florestal. In Republica Federal do Brasil: 1965; Vol. 4771.
8. Cochrane, T. T.; Cochrane, T. A., Diversity of the Land Resources in the Amazonian State of Rondônia, Brazil. *Acta Amazonica* **2006**, 36, (1), 91-102.
9. Zimmermann, B.; Elsenbeer, H.; De Moraes, J. M., The influence of land-use changes on soil hydraulic properties: Implications for runoff generation. *Forest Ecology and Management* **2006**, 222, 29-38.
10. ANA, Sistema de Monitoramento Hidrológico. In Agencia Nacional de Águas - ANA: 2009.
11. Martinelli, L. A.; Filoso, S., Expansion of Sugarcane Ethanol Production in Brazil: Environmental and Social Challenges. *Ecological Applications* **2008**, 18, (4), 885-898.
12. da Silva, A. M.; Casatti, L.; Alvares, C. A.; Leite, A. M.; Martinelli, L. A.; Durrant, S. F., Soil Loss Risk and Habitat Quality in Streams of a Meso-scale River Basin. *Scientia Agricola* **2007**, 64, (4), 336-343.
13. Butler, R. A., 55% of the Amazon may be lost by 2030 but carbon-for-conservation initiatives could slow deforestation. *Mongabay.com* January 23, 2008, 2008.
14. Sills, E. O.; Caviglia-Harris, J. L., Evolution of the Amazonian frontier: Land values in Rondônia, Brazil. *Land Use Policy* **2008**, 26, 55-67.
15. Fearnside, P. M., *Human carrying capacity of the Brazilian rainforest*. Columbia University Press: New York, 1986; p xii, 293 p.
16. Fearnside, P. M., Human carrying capacity estimation in Brazilian Amazonia as a basis for sustainable development. *Environ. Conserv.* **1997**, 24, (3), 271-282.
17. Bonell, M.; Hufschmidt, M. M.; Gladwell, J. S., *Hydrology and water management in the humid tropics : hydrological research issues and strategies for water management*. Unesco ; Cambridge University Press: Paris, France  
Cambridge ; New York, NY, USA, 1993; p xviii, 590 p.
18. Scanlon, B. R.; Jolly, I.; Sophocleous, M.; Zhang, L., Global impacts of conversions from natural to agricultural ecosystems on water resources: Quantity versus quality. *Water Resources Research* **2007**, 43, (3).

19. Magrin, G.; Gay Garcia, C.; Cruz Choque, D.; Giménez, J. C.; Moreno, A. R.; Nagy, G. J.; Nobre, C.; Villamizar, A., Climate Change 2007: Impacts, Adaptation and Vulnerability. Contribution of Working Group 2 to the Fourth Assessment Report of the Intergovernmental Panel on Climate Change. In *Fourth Assessment Report of the Intergovernmental Panel on Climate Change*, Parry, M. L.; Canziani, O. F.; Palutikof, J. P.; van der Linden, P. J.; Hanson, C. E., Eds. 2007; pp 582-607.
20. Svoray, T.; Shafran-Nathan, R.; Henkin, Z.; Perevolotsky, A., Spatially and temporally explicit modeling of conditions for primary production of annuals in dry environments. *Ecological Modelling* **2008**, *218*, (3-4), 339-353.